



Thermal and hydraulic performance of a heat exchanger working with carbon-water nanofluid

M. M. Sarafraz¹ · M. Silakhori¹ · S. A. Madani² · M. V. Kiamahalleh³ · O. Pourmehran¹

Received: 16 October 2018 / Accepted: 28 May 2019
© Springer-Verlag GmbH Germany, part of Springer Nature 2019

Abstract

In the present paper, the heat transfer and fluid flow characteristics of a copper-made heat exchanger were experimentally studied. The configuration of the heat exchanger was a double pipe and carbon-water nanofluid was utilised as a heat-exchanging medium within the heat exchanger. Experiments were conducted at volume fractions 0.1–1% and Reynolds number 800–10500. Plausible effect of various parameters including the nanofluid flow rate, nanoparticles' volumetric concentration and film temperature on the overall heat transfer coefficient (HTC) were investigated. Results showed that carbon/water nanofluid can offer a great potential for cooling applications. It was found that the flow rate of nanofluid; concentration and temperature of nanofluid can enhance the HTC. Interestingly, the presence of carbon nanoparticles within the base fluid resulted in the augmentation of pressure drop. This was because of the enhancement in friction factor parameter between layers of the base fluid and the augmentation in fluid viscosity, which is attributed to the presence of nano-carbons, which increased the pressure drop. Significant improvement in overall HTC was registered (44% enhancement) achieved at vol.% = 1. The penalty of 14% was reported for the pressure drop at vol.% = 1, which offers a trade-off between the increase in the value of HTC and augmentation in the value of pressure drop. The maximum value for thermal hydraulic performance of the system was 42.2% at Reynolds number 10200 and vol.% = 1.

1 Introduction

Process intensification and enhancement of thermo-hydraulic performance of heat exchanging systems is receiving attention in recent years [1–4]. Heat exchangers are most common used devices in heating and cooling systems with wide range of applications in industrial sectors such as automotive, pharmaceuticals and chemical processes. One of the significant challenges of heat exchangers is the poor thermal and physical properties of the coolants used in these systems, which limit

their applications. This challenge is associated with the poor thermal conductivity of the working fluids [5–8]. Thereby, much effort has been made to enhance the thermal performance of a heat exchanger by applying the process intensification to the system. Process intensification is a chain of techniques and methods to enhancement the thermal and hydraulic performance of systems [9–16]. Thus, the effort falls into two groups of passive and active process intensification techniques. Extension of heat-exchanging surface area is the most favourable passive technique; however, space limitation is still considered as the main drawback of this method. Advanced thermal engineered fluids such as nanofluids has been first utilised by Choi et al. [17]. Nanofluid is a colloidal mixture of conductive particles with average size of <100 nm dispersed in a base fluid such as deionized water.

Nanofluid can be used for augmenting the thermal properties of base fluid. As nanofluids are relatively cost-effective passive technique, easy to produce and less challenging in comparison with micro-fluids, therefore, they have been explored in many experimental studies [18–23]. For example, the heat transfer characteristics of water-based alumina nanofluid was investigated by Ryzhkov and Minakov [24]. Results showed that the considerable performance of the test

Nomenclature All parameters have already been defined within the text.

✉ M. M. Sarafraz
mohamadmohsensorsarafraz@gmail.com

- ¹ School of Mechanical Engineering, University of Adelaide, Adelaide, South Australia, Australia
- ² Department of Mechanical Engineering, Iran University of Science and Technology, Tehran 16765-163, Iran
- ³ Department of Mechanical Engineering and Advanced Material Research Centre, University of Malaya, 50603 Kuala Lumpur, Malaysia

nanofluid comparing to the base fluid such as low inlet viscosity and pumping power. However, considering the augmentation in pumping power, no systematic comparison was performed on thermal performance of the system. The effect of various parameters such as temperature on the HTC of alumina–water nanofluid in a copper-made tube was experimentally investigated by Ho and Lin [25]. Results demonstrated that nanofluids enhanced the thermo-physical properties together with HTC. This showed that alumina water has a great potential to be used as a coolant. Overall enhancement of 44% was reported for the HTC.

In another study, Bahiraei and Hangi [26] investigated the potential application of aqueous Mn/Zn nano-suspension in a heat exchanger. They investigated the influence of various operating parameters such as particle distribution size, concentration and the scale of magnetic field on the value of pressure drop and demonstrated anomalous improvement in heat transfer within the heat exchanging medium. These parameters were also studied in another work conducted by Wu et al. [27]. According to their results, there was no significant improvement in heat transfer for different regimes including laminar and turbulent flows. It means that the HTC increased up to 3.43% over the base fluid.

Somewhere else, enhancement of the HTC in a helical heat exchanger was reported to be 10.7% for vol.% = 0.02 for TiO₂/water over the base fluid, (water) [28]. In another works conducted by Sarafraz et al. [29–33], the HTC was shown to be decreased in forced convective heat transfer domain and nucleate boiling regime. They used CuO/water nanofluid around a vertical cylinder and investigated the potential effect of different operating parameters on HTC. In other works, they assessed the two-phase heat transfer characteristics of nanofluids and reported that nanofluids might not suitable for the boiling heat transfer regimes [34–37]. In contrast to Sarafraz et al.'s work, in another similar experiments, Darzi et al. [23] showed that the addition of nanoparticles enhances the properties of base fluid in a way that the nano-suspension can have a plausible applications in cooling systems. Sahin et al. [38] studied the convective HTC together with the value for the pressure drop under the turbulent regime. The aqueous mixture of alumina and water was used as a working fluid. They showed that the HTC can be enhanced increased with an increase in the fluid flow rate, and the concentration of particle. They did not report any specific information on the pressure drop of the system. Wang et al. [39] examined the laminar forced convection of carbon nanotube nanofluid in a horizontal circular tube. They reported that at $Re > 100$, Nu number significantly augmented with an increase in Re number, that shows the convective heat transfer enhancement is not only due to the enhancement in thermal conductivity. Fazeli et al. [40] presented the experimental results of heat transfer and pressure drop of laminar flow of nanofluids containing Silica nanofluids in a miniature heat sink. They found that the SiO₂/

water nanofluids enhanced the HTC while also showed a 10% decrease in the thermal resistance of the heat sink.

Amongst the various nanofluids assessed for thermal engineering applications, carbon nanoparticle is a relatively new nanomaterial, which is cheap and easy-to-fabricate material with relatively high thermal conductivity (e.g. ~3200 W/(mK)). Search the literature, it can be understood that carbon nanoparticle is widely used for the absorption and water treatment, however, such a plausible thermal conductivity can potentially be used for thermal applications. Hence, the novelty of the present work is to use carbon nanoparticles to improve the thermal performance of the system. As carbon nanoparticle is a cheap material, it can further improve the economic viability of the process as well. Thus, in the present work, an experimental investigation is conducted on the potential application of the spherical carbon nanoparticles/water in a heat exchanger with double pipe configuration. Characterization of the carbon nanoparticles including pore size distribution, x-ray diffraction test, transmission electron microscopic image and particle size test is performed. Assessment of thermal and physical properties of nanofluid including thermal conductivity, specific heat, viscosity and density of nanofluid is experimentally conducted and briefly discussed. The test enable one to investigate the influence of different operating parameters such as volumetric concentration of nanoparticles, flow rate of nanofluid, temperature of nanofluid on overall HTC and pressure drop.

2 Experimental

2.1 Test rig

Figure 1 shows a schematic representation of the test rig used in the present research. The test rig has three main units including the main test section (double pipe heat exchanger), measurement instruments including thermocouples, flow meter and pressure transmitters and cooling/hot loops for circulating the nanofluid and water. The test section is a double pipe heat exchanger consisting of two tubes with nominal diameter of 6.35 mm and 12.7 mm, for inner and outer tubes. The pipes were fabricated from copper. Nanofluid was introduced to the inner tube, while water at 20 °C was used inside annular space. The body of the heat exchanger was heavily isolated to minimise the heat loss to environment. Cooling loops include the tubes and two centrifugal pumps manufactured by DAB Co. to pump the nanofluid and water to the heat exchanger. Nanofluid was carbon/water and was prepared using two-step method described in the following section. Distillate water was also chilled using a refrigerant thermostat bath. To measure the flow rate within the loops, an ultrasonic flow meter was employed manufactured by Flownetix (0–50 lpm). It was calibrated for nanofluid using

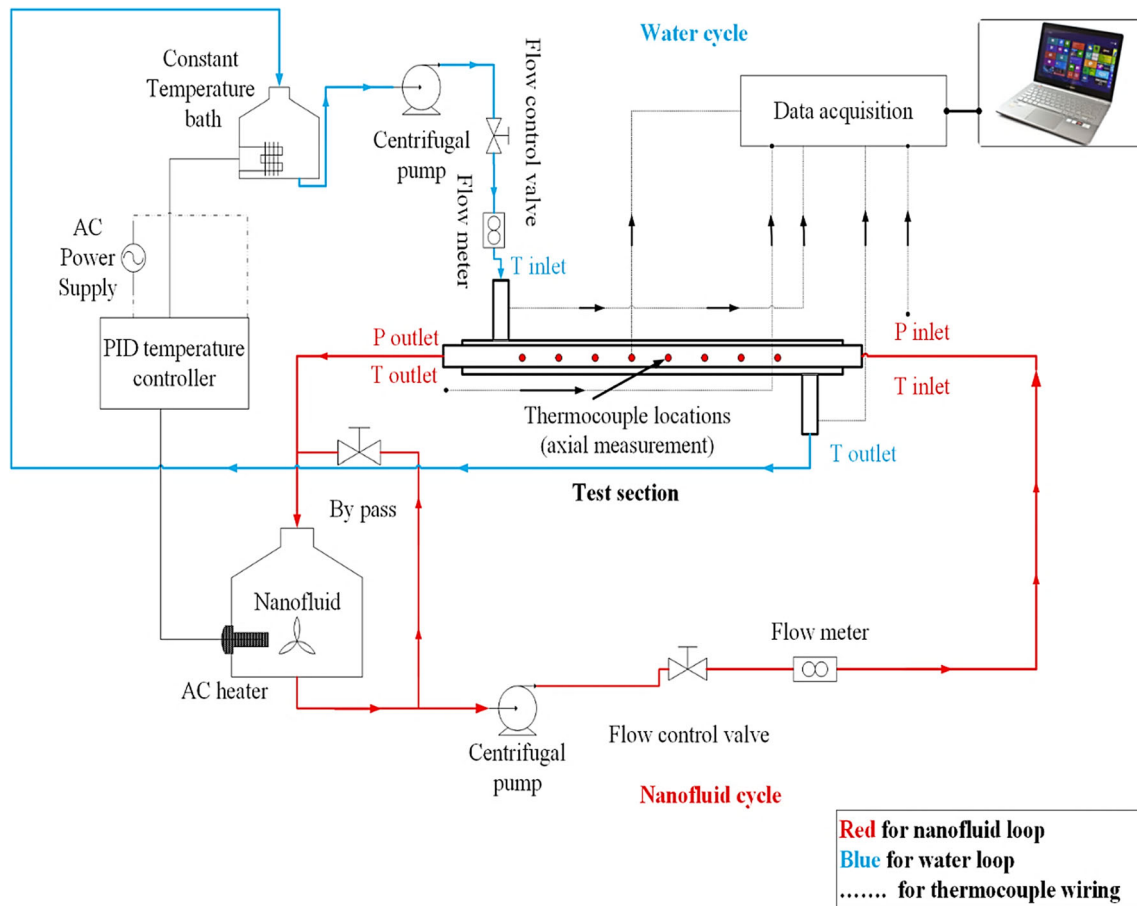


Fig. 1 A schematic representation of test setup employed in this study

a particulate fluid calibrator. To control the temperature of the tank a cartridge heater connected to an AC transformer was employed. The cut-off circuit was controlled with a PID controller not only to maintain a constant temperature to the nanofluid tank, but also to prevent from evaporation of the nanofluid. The nanofluid tank was kept at 40–70 °C. All the pipes, joints and tanks were heavily insulated using glass wool. To measure the temperatures of fluids, four thermocouples were placed at the inlet section and outlet section of the heat exchanger. The temperature readings were set to a data logger to monitor the temperature data with data reading frequency of 1 kHz. To measure the axial temperature profile along with the heat exchanger, eight thermocouples were mounted on the exterior wall of the inner tube. Also, to measure the inlet and the outlet temperature of the inner tube, two thermocouples were installed at the inlet and the outlet port of the inner tube. To eliminate the potential effect of thermal resistance, a T18 silicon paste was used in thermowells. To assess the value of the pressure drop within the heat exchanger, two pressure transmitters manufactured by OMEGA were mounted at inlet and outlet of the test section. Detailed specification of the experimental instruments have been given in Table 1.

2.2 Materials and characterization of nanofluid

Carbon nano-powder (CNP), (Sigma-Aldrich, USA) was used as the carbon-based nanoparticle source. Nitrogen adsorption test was carried out to measure and estimate the surface area and size distribution of particle (PSD) of the carbon nanoparticles and is shown in Fig. 2. The higher surface area, the higher thermal performance is expected to achieve. Results showed that samples have mesoporous structure with negligible contributions from microspores. The results of the particle size distribution test for the CNP sample is shown in Fig. 3. The distribution is multimodal, showing a broad range of 4–50 nm. The intensity of the distribution curve is very small. This low intensity and broad distribution of pores confirm that the available surface area is primarily due to the particle's external surface rather than their internal porosity.

X-ray diffraction test was employed using GNR APD instrument. The data were recorded in continuous scan mode and with the step size of 0.02° and at the range of 2–80° [42]. As can be seen in Fig. 4, the XRD pattern reveals that the characteristic peaks are seen in 26°, 43° and 55°, which are the characteristic peaks of the carbon material. Also, there is no other peaks in the XRD sample. This implies that the

Table 1 Uncertainties of the devices utilised for the experimental measurements

Instrument	model	Accuracy
Ultrasonic tracking flowmeter	US100 X Flow-netix	$\pm 1\%^0$
Thermocouple	K-type, Omega	$\pm 0.1 \text{ K}^*$
Cartridge heater	1200 W, 100mm \times 10mm(L \times D)	$\pm 1.5\%^*$
Pump	Centrifugal	–
Pressure transmitter	Sensys PT	$\pm 1\%^*$
PID	Autonics	$\pm 1\%^0$

*estimated with calibration procedure, ⁰based on the manufacturer claim

structure of the carbon is pure and then the thermal conductivity of the particles is the same. Also, there is no noise in the result of the XRD showing that the particles are almost uniform in terms of size and morphology.

To assess the morphology, dispersion and agglomeration, Scanning Electron Microscopic image (SEM, represented in Fig. 5a) and Transmission Electron Microscopic images, (TEM) were provided by Tecnai, G2 spirit TEM, USA; and from a sample of 1% by volume of carbon nanoparticles inside the deionized water as represented in Fig. 5b. As can be seen, the morphology is spherical and the same for the particles. Importantly, neither cluster nor agglomeration is formed during the dispersion.

Figure 6 presents the experimental results obtained for the particle size sampling for carbon nanoparticles. Analysis of particle size test showed that the average particle size for carbon nanoparticles is 50 nm, which is in accordance with the results obtained by scanning electron microscopic and transmission electron microscopic images. To ensure about the repeatability of the particle size test, measurements were conducted three times and results were consistent.

2.3 Data reduction

To measure the HTC in the hot loop, following correlations:

$$Q_{nf}^{hot} = m_{nf} \cdot C_{p,nf} (T_{in,nf} - T_{out,nf}) \quad (1)$$

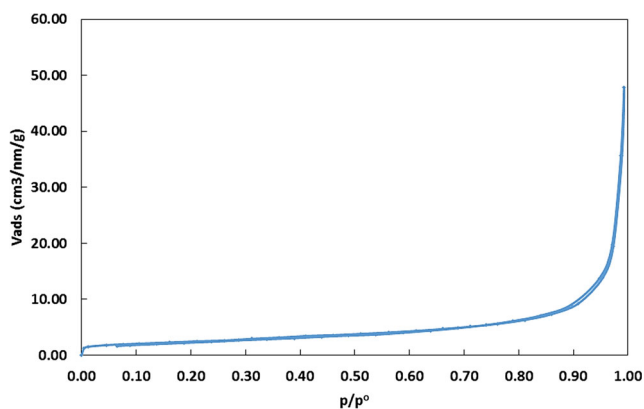


Fig. 2 Nitrogen adsorption isotherm on CNP sample [41]

For the cooling loop, following equation was implemented:

$$Q_w^{cold} = m_w \cdot C_{p,w} (T_{in,w} - T_{out,w}) \quad (2)$$

Here, Q_{nf}^{hot} is heat transfer of in hot loop and m_{nf} is its mass flow rate. Likewise, Q_w^{cold} is heat transfer in cooling loop and m_w is its mass flow rate. Thereby average rate of heat transferred between inner and outer pipes can be estimated with the following equation:

$$Q_{ave} = \frac{Q_{nf}^{hot} + Q_w^{cold}}{2} \quad (3)$$

To calculate the HTC of hot loop, h , Eq. (4) was utilised:

$$h_{nf} = \frac{Q_{ave}}{T_w - T_{b,nf}} \quad (4)$$

Here, T_w is the average of temperature reading from the wall mounted thermo-meters. T_b is bulk temperature calculating from the average of inlet and outlet temperatures of inner tube. The dimensionless numbers employed in the present research were Prandtl Nusselt, Pecklet and Reynolds numbers as follows:

$$Nu_{nf} = \frac{h_{nf} \cdot D_i}{k_{nf}} \quad (5)$$

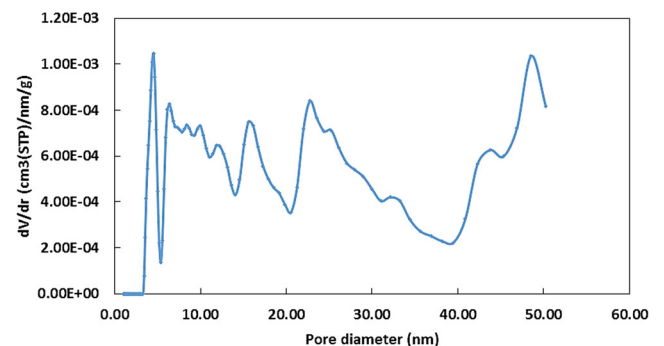


Fig. 3 The estimated distribution of pore size (PSD) according to QSDFT for CNP sample [41]

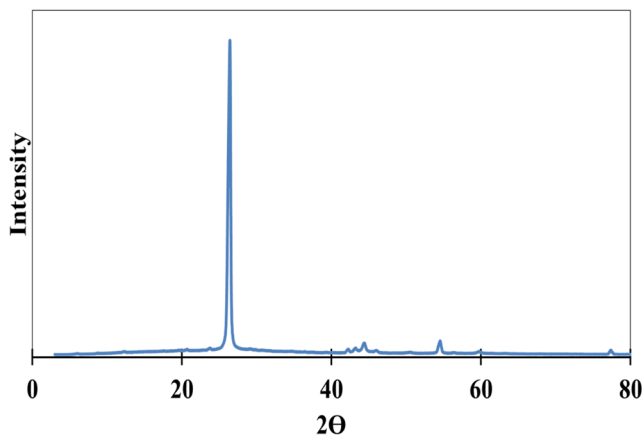


Fig. 4 Results of XRD test conducted on carbon nanoparticles

$$Re_{nf} = \frac{\rho_{nf} \cdot u_{nf} \cdot D_i}{\mu_{nf}} \quad (6)$$

$$Pe_{nf} = \frac{u_m \cdot d_p}{\alpha_{nf}}, \quad \alpha_{nf} = \frac{k_{nf}}{\rho_{nf} C_{p,nf}} \quad (7)$$

$$Pr_{nf} = \frac{C_{p,nf} \cdot \mu_{nf}}{k_{nf}} \quad (8)$$

Also important is to estimate the friction factor which may be intensified due to the presence of nanoparticles. Following equation was used:

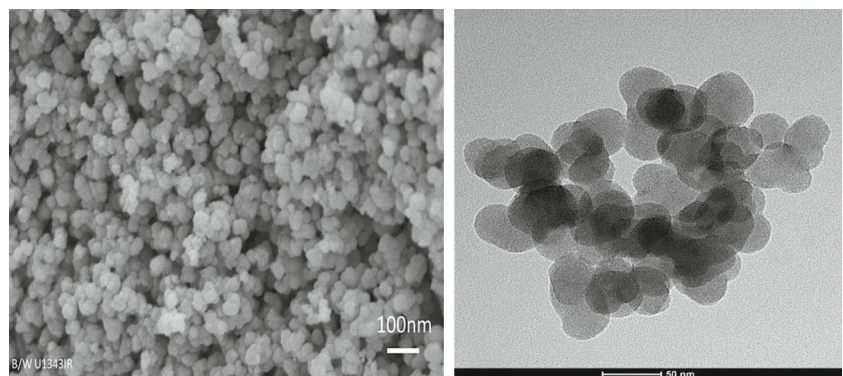
$$f = \frac{\Delta p}{l_e \cdot \frac{2G^2}{D_{hyd} \cdot \rho}} \quad (9)$$

Here, L is the length in which fluid is flowing, G is the velocity (mass based, multiplication of density, ρ and volumetric flow); Δp is the value of the pressure drop.

Thermal performance is estimated with the following equation:

$$\eta = \left(\frac{Nu_{nf}}{Nu_{bf}} \right) \cdot \left(\frac{f_{bf}}{f_{nf}} \right)^{\frac{1}{3}} \quad (10)$$

Fig. 5 **a** Scanning electron microscopic image of carbon nanoparticles [41]. **b** TEM image of carbon nanoparticles dispersed in deionized water [41]



a Scanning electron microscopic image of carbon nanoparticles.

b TEM image of carbon nanoparticles dispersed in deionized water.

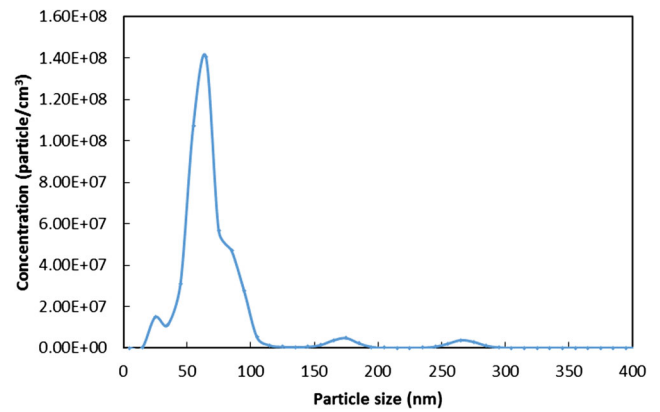


Fig. 6 Results of particle size test for carbon nanoparticles

f is the friction factor and nf , bf stands for nanofluid and base fluid, respectively. Uncertainty was estimated using the method introduced by Moffat [43]. The total uncertainty for this experiment based on Table 1 was estimated to be about 9.1%. to ensure about the uncertainty, results were checked by Kline-McClintock's equation [44]. The total uncertainty estimated for the heat loss was 5.1%, and for Reynolds number was 8.2%, while it was 10.1% for overall HTC and 9.2% for pressure drop. These estimations were double-checked with the equation introduced by Moffat et al. [40]. A fair agreement between the data and the correlation ($\sim 8\%$ deviation) was obtained.

2.4 Thermal and physical properties of nano-suspensions

Since thermal and physical properties of the nanofluids are critical, therefore, they were experimentally obtained. As shown in Fig. 7, thermal conductivity is enhanced with an increase in the concentration of nanofluid. For better understanding, comparison was made between water and nanofluid. At vol.% = 1, 15% enhancement was seen in thermal conductivity of water. This can be attributed to the Brownian motion of the NPs and thermo-phoresis phenomenon intensified at

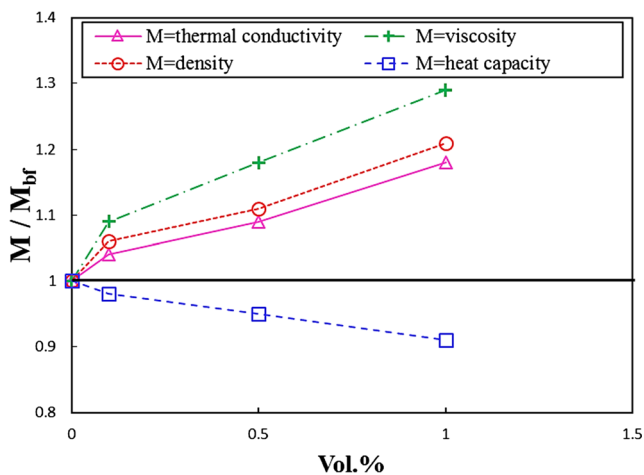


Fig. 7 Thermo-physical properties of carbon aqueous nanofluid

60 °C. Interestingly, density of nanofluid is also larger than that of measured for water. This is clearly due to the presence of nanoparticles, which increases the mass of the base fluid per unit of the volume. Note that, KD2 Pro Decagon was implemented to measure the thermal conductivity of nanofluids.

Viscosity was measured with Brookfield digital viscometer. It was found that with an increase in the volumetric concentration of nanoparticles, the viscosity of nanofluid increased. This was attributed to the friction forces and friction forces between layers of the fluid. The heat capacity of nanofluid decreased with an increase in the volumetric concentration of CNPs. This is because the heat capacity of carbon nanoparticles is several times lower than water. Density was measured with Anton Paar densitometer device. Notably, the heat capacity was measured with thermo-gravimetric device.

2.5 Calibration and validation of the experimental setup

It is necessary to calibrate and to valid the test rig to ensure about the accuracy of the experimental data. For this purpose, deionized water was used for the test and the obtained results were examined against the well-known correlations such as Gnielinski and Dittus-Boelter correlations for both laminar and turbulent regions. According to Fig. 8, the HTC obtained by the correlations is in a reasonable agreement with those of experimentally obtained. As expected, with an increase in the flow rate of the working fluid, the HTC value increases and both correlations show the same accuracy for predicting the HTC. However, For low Reynolds numbers, due to the increase in the residence time of the fluid inside the heat exchanger, the heat loss increases resulting in a small mismatch between the results calculated by the correlations and those of experimentally obtained. However, this deviation is still less than 11%–13.8% and is only seen for $1000 < Re < 1500$.

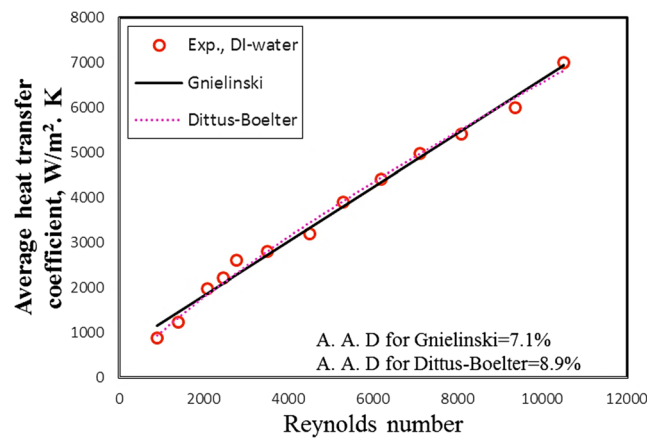


Fig. 8 Dependence of HTC on the Re number of the fluid during the calibration test for deionized water

Therefore, results are reliable and experiments can be conducted for the nanofluids.

The friction factor of the system was also measured for water as a reference case. The results were compared to Colebrook's equation. As shown in Fig. 9, results are in a fair agreement with the well-known Colebrook equation and data are reliable. As shown, the friction factor decreases non-linearly with an increase in the value of Reynolds number and close to the values estimated by Colebrook equation. Therefore, the experimental setup can measure the pressure drop and friction factor accurately.

3 Results and discussions

3.1 Flow rate of fluid

Figure 10 shows the dependence of HTC on Re of the nanofluids for various volumetric fractions and for DI water at temperature 50 °C. With an increase in Re, the HTC

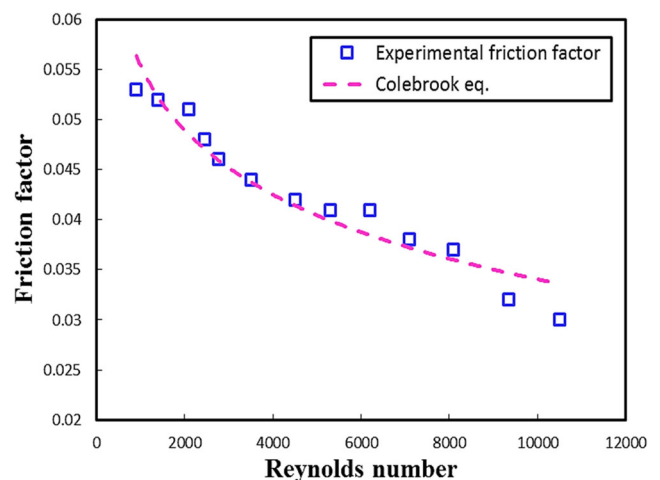


Fig. 9 Dependence of friction factor of deionized water on the Reynolds number at temperature 50 °C

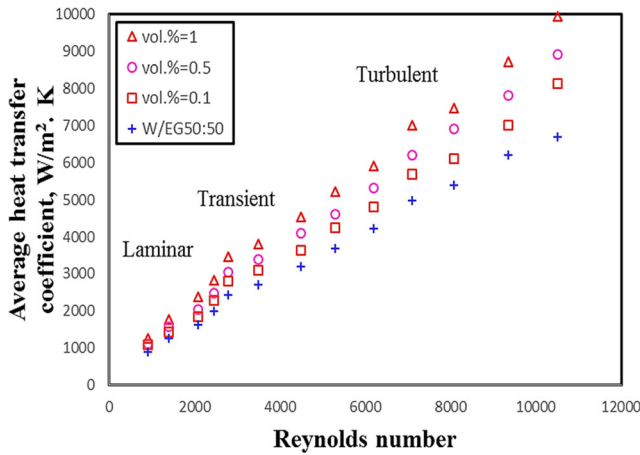


Fig. 10 Influence of flow rate of nanofluids on the HTC

increases for all concentrations and even the base fluid. More importantly, when volumetric concentration of nanoparticles increases, the HTC is increased too. This trend was seen for all three flow regimes including laminar, transient and turbulent, however, in turbulent region the HTC is ~10 times larger than that of obtained for the laminar domain. This is because of the intensification of the Brownian motion, agitation and eddies, which intensifies the heat transfer rate inside the heat exchanging media. Similar trends were seen for other temperatures; while the quantity of the HTC was increased at higher temperatures, which is discussed later.

For better representation of the results, enhancement parameter is defined as follows:

$$Enhancement\ parameter = \frac{U_{nf}}{U_{bf}} \quad (11)$$

In which, U is the HTC ($W/m^2 \cdot K$), for nanofluid (nf) and base fluid (bf). Figure 11 shows the variation of enhancement ratio with the concentration and different volumetric fraction of the nanofluids. According to the represented results in Fig. 11, enhancement parameter increases with an increase

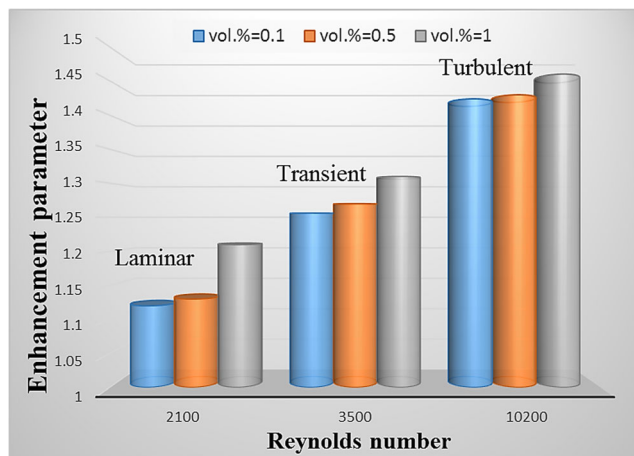


Fig. 11 Variation of enhancement parameter with Reynolds number

the Reynolds number meaning that carbon nanofluid can work at high flow rates as they present higher HTC. Noticeably, for the laminar region, enhancement parameter is still higher than 1, which means that the HTC enhances at Reynolds $0 < Re < 2300$. This enhances the span of application of carbon nanofluids at low flow rate conditions. For concentration, the HTC is intensified when flow rate increases.

A comparison was made between the experimental data and those of theoretically calculated from the well-known correlations not only to validate the experimental data, but also to see if the well-known correlations can estimate the HTC of nanofluid. Figure 12 shows the results of a comparison between the experimental data and those of obtained with well-known correlations such as Pak and Cho, Gnielinski, Maiga et al. and Xuan-Li correlations [45]. Results of the comparison revealed that the HTC values are in a good agreement with the correlations. According to the figure, the experimental HTC values are within $\pm 30\%$ against the correlations. Also, for most of the experimental data, the absolute average deviation was $\pm 15\%$.

3.2 Concentration of carbon nanoparticles

Figure 13 presents the potential effect of volumetric fraction of carbon nanoparticles HTC at various Reynolds number. Reynolds number were chosen in a way that three flow regimes of laminar, transient and turbulent were considered. As shown in Fig. 12, by increasing in volumetric fraction of carbon NPs, the HTC is enhanced. For instance, at $vol.\% = 0.1$ the HTC is 2240, while it is 2480 and 2790 for $vol.\% = 0.5$ and $vol.\% = 1$, respectively. However, system showed that the HTC is very sensitive to flow rate rather than concentration of carbon nanoparticles. For example, at Reynold number = 2500, the $HTC = 2790 (W/m^2 \cdot K)$, for nanofluid (at $vol.\% = 1$), while it is $9800 (W/m^2 \cdot K)$, at $Re = 10,500$. This is because

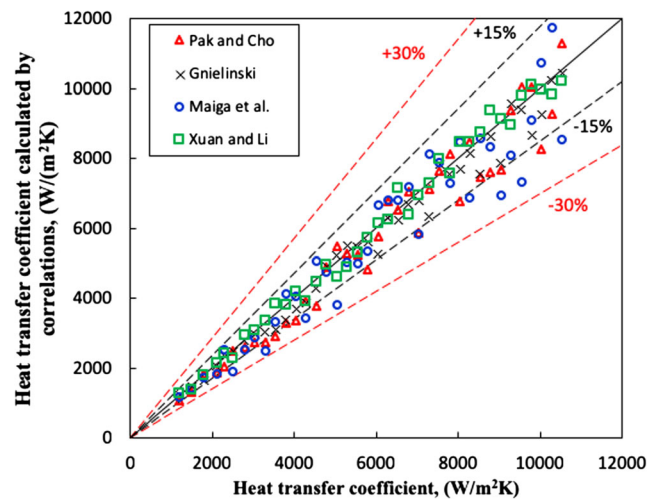


Fig. 12 Results of a comparison between the HTC value and those of calculated with the correlations

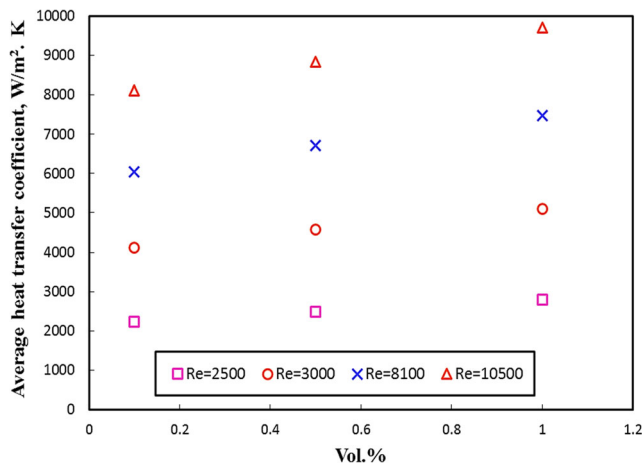


Fig. 13 Variation of volumetric fraction of nanofluid on HTC of nanofluids

of the low thermal conductivity of carbon nanoparticles as with increasing the concentration of nanoparticle, thermal conductivity of the nanofluid is enhanced 15% at maximum vol.% = 1. The HTC value obtained in this work was relatively larger than those of reported for other nanofluids and pure liquids [46–49].

3.3 Inlet temperature

Figure 14 shows the influence of Reynolds number on overall HTC at various mean temperature of hot loop (inlet temperature) to the heat exchanger. Results demonstrated that by increasing the mean inlet temperature of nanofluid, the HTC is enhanced and the increase follows a rectilinear trend. This trend can be seen for all other volumetric concentrations and at any Re numbers. This is simply because an increase in the temperature of the nanofluids can improve viscosity, thermal conductivity, density and heat capacity of nanofluid. Noticeably, impact of temperature on the HTC is insignificant

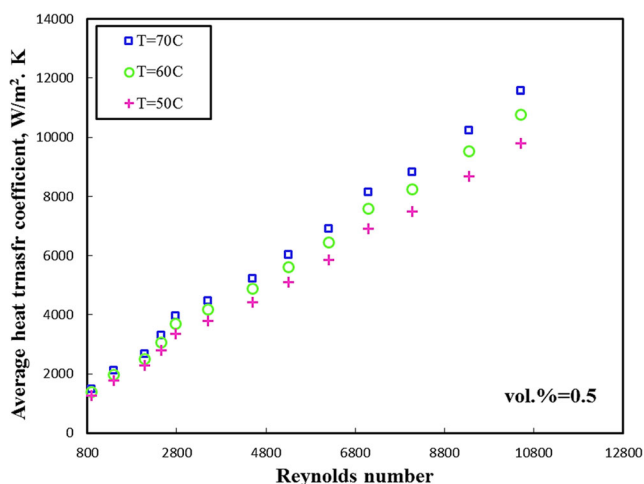


Fig. 14 Variation of inlet temperature of hot loop on overall HTC of nanofluids

in laminar and to some extent in transient flow regimes, however, it significantly improves the HTC in turbulent region.

3.4 Pressure drop

Figure 15 represents the values of pressure drop obtained at different flow rate of carbon nanofluids at temperature 60 °C. According to Fig. 14, by increasing the flow rate of nanofluid, pressure drop linearly increases, while the pressure drop for turbulent flow rates are considerably higher than laminar regime. Since only single-phase heat transfer occurs inside the heat exchanger, eddies and friction of fluid in contact with the inner pipe walls are responsible for the pressure drop. More importantly, presence of carbon nanoparticles inside the heat exchanger intensifies the pressure drop because particles increase the viscosity of the coolant as well. At Reynolds number of 910, pressure drop is 150% lower than the value measured at Reynolds number 3500, meaning that pressure drop is strongly dependent to the flow rate of nanofluid. For deionized water, similar trend is seen. For the Reynolds number of 900 at vol.% = 1, pressure drop is 133% lower than that of measured at Reynolds number 3500. Meaning that pressure drop is higher in comparison with DI water at a given Reynolds number, which is due to the interaction of particles, base fluid and the heat exchanger walls.

Figure 16 presents the change in values of pressure drop due to the variation of Reynolds number in turbulent region and for various volumetric fraction of carbon NPs. With an increase in the flow rate, the value for the pressure drop increases. Also, increasing the volumetric fraction of NPs results in the augmentation of pressure drop. For instance, at vol.% = 1 and at Reynolds number 10500, the pressure drop is 10.5, while it is only 2 at Re = 4500.

For better understanding, a comparison is made between the experimental friction factor obtained for nanofluids and the base fluid. According to Fig. 17, adding the nanoparticles into the base fluid increases the value of the friction factor. For

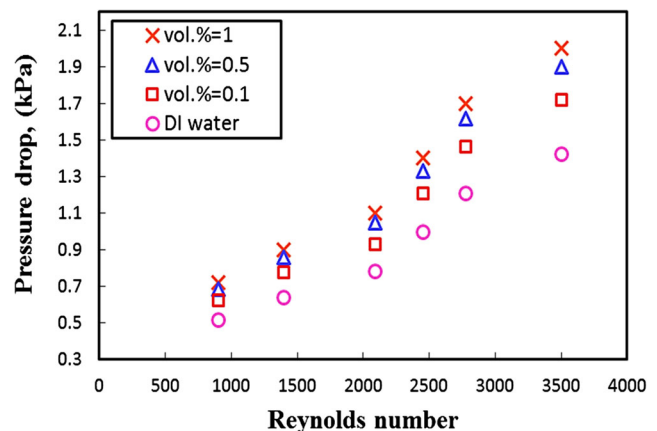


Fig. 15 Dependence of pressure drop on fluid flow rate of nanofluids and base fluid in laminar regime

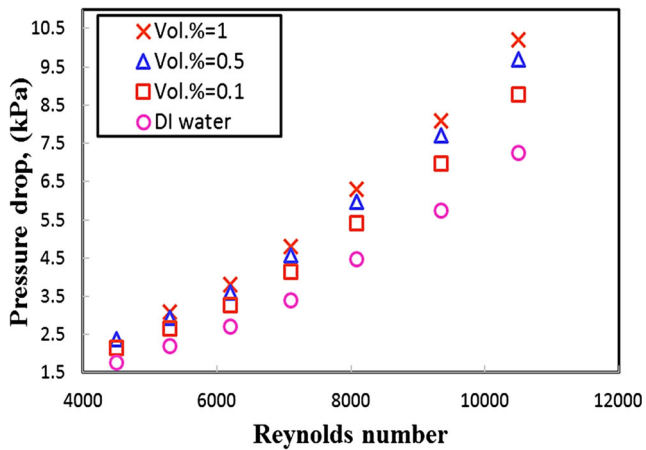


Fig. 16 Variation of pressure drop values with Re in turbulent regime and for various volumetric fractions of nanofluid

vol.% = 0.1, the friction factor increases by 2%, while for vol.% = 0.5 and 1%, it increases 9 and 14%, respectively. Presence of nanoparticles can increase the probability of sticking of particles on the walls of the inner tube which enhances the values of pressure drop. Notably, enhancement in viscosity also results in the augmentation in the friction factor and pressure drop.

3.5 Overall thermal performance

Figure 18 shows the variation of thermo-hydraulic performance of the nanofluid on the volumetric fraction of nanofluids. As can be seen, even though friction factor is enhanced with an increase in the volumetric fraction of nanofluid, the thermo-hydraulic performance of the system still increases. This is because enhancement in the HTC is more effective than the enhancement in the pressure drop. In fact, there is a trade-off between the HTC enhancement and pressure augmentation. For the carbon/water nanofluid, the

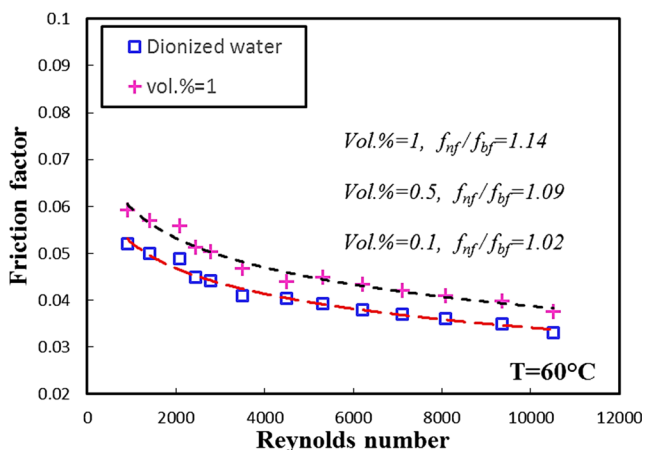


Fig. 17 Experimental friction factor of DI water and carbon nanofluid at vol.% = 1 and at temperature 50 °C. As results almost overlapped each other, for other concentration the average friction factor enhancement was reported

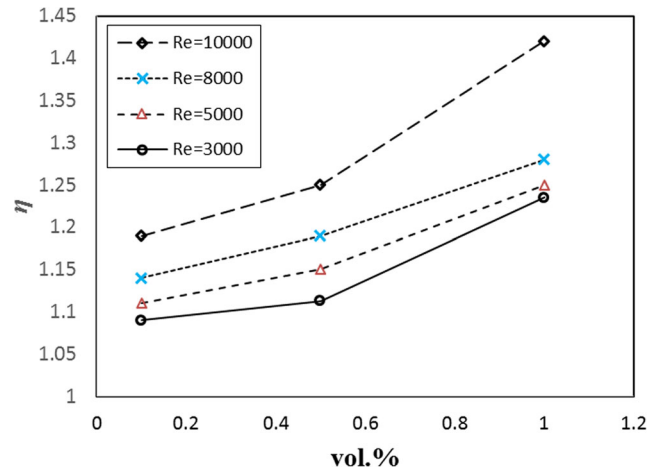


Fig. 18 Thermal performance of the system at different volume fractions of nanofluids and for different Reynolds number

experiments show that the HTC enhancement is the determining factor. In other words, carbon nanoparticle can enhance the thermal performance of the system by intensifying the convective HTC within the heat exchanger. Also, at higher Re numbers, thermo-hydraulic performance of the system is more intensified in comparison with mid-range and low Reynolds numbers. This is because of the formation of eddies, Brownian motion of nanoparticles, local agitation of fluid, thermo-phoresis effect and flow regime.

4 Conclusion

In this study, some experiments were conducted to evaluate the convective thermal performance of carbon/water nanofluid in a double pipe heat exchanger. Following conclusions were drawn:

- Experimental measurements on thermo-physical properties showed that carbon nanoparticles can improve the thermal conductivity, viscosity and density of nanofluid up to 30%, 20 and 16% respectively at vol.% = 1.
- Carbon nanoparticles in deionized water can enhance the convective HTC up to 45% at vol.% = 1. With an increase in concentration of particles, flow rate and inlet temperature of nanofluids, convective HTC is augmented.
- Presence of particles within the base fluid added a small penalty for the pressure drop due to the enlargement in the friction factor and viscosity of base fluid. However, this penalty is insignificant in comparison with 45% of enhancement in HTC.
- Although pressure drop and friction factor both increased slightly, the overall thermal performance of nanofluid within the heat exchanger increased. Moreover, by increasing the concentration of NPs, higher thermal

performance is achievable for the range of 0.1–1% by volume of nanoparticles.

Compliance with ethical standards

Conflict of interest The authors of the article declare that there is no conflict of interest between the authors or any third parties including institutions.

References

- Farajollahi B, Etemad SG, Hojjat M (2010) Heat transfer of nanofluids in a shell and tube heat exchanger. *Int J Heat Mass Transf* 53:12–17
- Mohammed HA, Bhaskaran G, Shuaib NH, Saidur R (2011) Heat transfer and fluid flow characteristics in microchannels heat exchanger using nanofluids: a review. *Renew Sust Energ Rev* 15: 1502–1512
- Li Q, Xuan Y (2002) Convective heat transfer and flow characteristics of Cu-water nanofluid. *Science in China Series E: Technological Science* 45:408–416
- Reddy MCS, Rao VV (2014) Experimental investigation of heat transfer coefficient and friction factor of ethylene glycol water based TiO₂ nanofluid in double pipe heat exchanger with and without helical coil inserts. *International Communications in Heat and Mass Transfer* 50:68–76
- Pandey SD, Nema VK (2012) Experimental analysis of heat transfer and friction factor of nanofluid as a coolant in a corrugated plate heat exchanger. *Exp Thermal Fluid Sci* 38:248–256
- Ghozatloo A, Rashidi A, Shariaty-Niassar M (2014) Convective heat transfer enhancement of graphene nanofluids in shell and tube heat exchanger. *Exp Thermal Fluid Sci* 53:136–141
- Zamzamin A, Oskouie SN, Doosthoseini A, Joneidi A, Pazouki M (2011) Experimental investigation of forced convective heat transfer coefficient in nanofluids of Al₂O₃/EG and CuO/EG in a double pipe and plate heat exchangers under turbulent flow. *Exp Thermal Fluid Sci* 35:495–502
- Garoosi F, Hoseininejad F, Rashidi MM (2016) Numerical study of heat transfer performance of nanofluids in a heat exchanger. *Appl Therm Eng* 105:436–455
- M. M. Sarafraz, Iskander Tlili, Mohammad Abdul Baseer, Mohammad Reza Safaei, (2019) Potential of Solar Collectors for Clean Thermal Energy Production in Smart Cities using Nanofluids: Experimental Assessment and Efficiency Improvement. *Applied Sciences* 9 (9):1877
- E. Salari, S. M. Peyghambarzadeh, M. M. Sarafraz, F. Hormozi, V. Nikkhab, (2017) Thermal behavior of aqueous iron oxide nanofluid as a coolant on a flat disc heater under the pool boiling condition. *Heat and Mass Transfer* 53 (1):265–275
- M.M. Sarafraz, H. Arya, M. Saeedi, D. Ahmadi, (2018) Flow boiling heat transfer to MgO-therminol 66 heat transfer fluid: Experimental assessment and correlation development. *Applied Thermal Engineering* 138:552–562
- M.M. Sarafraz, M. Arjomandi, (2018) Thermal performance analysis of a microchannel heat sink cooling with copper oxide-indium (CuO/In) nano-suspensions at high-temperatures. *Applied Thermal Engineering* 137:700–709
- M.M. Sarafraz, H. Arya, M. Arjomandi, (2018) Thermal and hydraulic analysis of a rectangular microchannel with gallium-copper oxide nano-suspension. *Journal of Molecular Liquids* 263:382–389
- M.M. Sarafraz, M. Arjomandi, (2018) Demonstration of plausible application of gallium nano-suspension in microchannel solar thermal receiver: Experimental assessment of thermo-hydraulic performance of microchannel. *International Communications in Heat and Mass Transfer* 94:39–46
- M.M. Sarafraz, S.M. Peyghambarzadeh, (2012) Influence of thermodynamic models on the prediction of pool boiling heat transfer coefficient of dilute binary mixtures. *International Communications in Heat and Mass Transfer* 39 (8):1303–1310
- Elham Salari, Mohsen Peyghambarzadeh, Mohammad Mohsen Sarafraz, Faramarz Hormozi, (2016) Boiling Heat Transfer of Alumina Nano-Fluids: Role of Nanoparticle Deposition on the Boiling Heat Transfer Coefficient. *Periodica Polytechnica Chemical Engineering* 60 (4):252–258
- Choi SUS, Zhang ZG, Yu W, Lockwood FE, Grulke EA (2001) Anomalous thermal conductivity enhancement in nanotube suspensions. *Appl Phys Lett* 79:2252–2254. <https://doi.org/10.1063/1.1408272>
- Hwang YJ, Ahn YC, Shin HS, Lee CG, Kim GT, Park HS, Lee JK (2006) Investigation on characteristics of thermal conductivity enhancement of nanofluids. *Curr Appl Phys* 6:1068–1071. <https://doi.org/10.1016/j.cap.2005.07.021>
- Aravind SSJ, Baskar P, Baby TT, Sabareesh RK, Das S, Ramaprabhu S (2011) Investigation of Structural Stability, Dispersion, Viscosity, and Conductive Heat Transfer Properties of Functionalized Carbon Nanotube Based Nanofluids. *J Phys Chem C* 115:16737–16744. <https://doi.org/10.1021/jp201672p>
- Duangthongsuk W, Wongwises S (2008) Effect of thermophysical properties models on the predicting of the convective heat transfer coefficient for low concentration nanofluid. *International Communications in Heat and Mass Transfer* 35:1320–1326. <https://doi.org/10.1016/j.icheatmasstransfer.2008.07.015>
- Das SK, Putra N, Roetzel W (2003) Pool boiling characteristics of nano-fluids. *Int J Heat Mass Transf* 46:851–862. [https://doi.org/10.1016/S0017-9310\(02\)00348-4](https://doi.org/10.1016/S0017-9310(02)00348-4)
- Tiwari AK, Ghosh P, Sarkar J (2013) Heat transfer and pressure drop characteristics of CeO₂/water nanofluid in plate heat exchanger. *Appl Therm Eng* 57:24–32
- Darzi AAR, Farhadi M, Sedighi K (2013) Heat transfer and flow characteristics of Al₂O₃–water nanofluid in a double tube heat exchanger. *International Communications in Heat and Mass Transfer* 47:105–112
- Ryzhkov II, Minakov AV (2014) The effect of nanoparticle diffusion and thermophoresis on convective heat transfer of nanofluid in a circular tube. *Int J Heat Mass Transf* 77:956–969. <https://doi.org/10.1016/j.ijheatmasstransfer.2014.05.045>
- Ho CJ, Lin YJ (2014) Turbulent forced convection effectiveness of alumina–water nanofluid in a circular tube with elevated inlet fluid temperatures: An experimental study. *International Communications in Heat and Mass Transfer* 57:247–253. <https://doi.org/10.1016/j.icheatmasstransfer.2014.08.017>
- Bahiraei M, Hangi M (2013) Investigating the efficacy of magnetic nanofluid as a coolant in double-pipe heat exchanger in the presence of magnetic field. *Energy Convers Manag* 76:1125–1133
- Wu Z, Wang L, Sundén B (2013) Pressure drop and convective heat transfer of water and nanofluids in a double-pipe helical heat exchanger. *Appl Therm Eng* 60:266–274
- Chandra Sekhara Reddy M, Vasudeva Rao V (2014) Experimental investigation of heat transfer coefficient and friction factor of ethylene glycol water based TiO₂ nanofluid in double pipe heat exchanger with and without helical coil inserts. *International Communications in Heat and Mass Transfer* 50:68–76. <https://doi.org/10.1016/j.icheatmasstransfer.2013.11.002>
- Sarafraz MM, Hormozi F (2014) Scale formation and subcooled flow boiling heat transfer of CuO–water nanofluid inside the vertical annulus. *Exp Thermal Fluid Sci* 52:205–214. <https://doi.org/10.1016/j.expthermflusci.2013.09.012>

30. Sarafraz MM, Hormozi F (2014) Convective boiling and particulate fouling of stabilized CuO-ethylene glycol nanofluids inside the annular heat exchanger. *International Communications in Heat and Mass Transfer* 53:116–123. <https://doi.org/10.1016/j.icheatmasstransfer.2014.02.019>
31. Sarafraz M, Peyghambarzadeh S, Alavi Fazel S, Vaeli N (2013) Nucleate pool boiling heat transfer of binary nano mixtures under atmospheric pressure around a smooth horizontal cylinder
32. Sarafraz MM, Hormozi F, Peyghambarzadeh SM, Vaeli N (2015) Upward Flow Boiling to DI-Water and CuO Nanofluids Inside the Concentric Annuli. *Journal of Applied Fluid Mechanics* 8
33. Sarafraz MM, Nikkhah V, Madani SA, Jafarian M, Hormozi F (2017) Low-frequency vibration for fouling mitigation and intensification of thermal performance of a plate heat exchanger working with CuO/water nanofluid. *Appl Therm Eng* 121:388–399
34. Sarafraz MM (2013) Experimental investigation on pool boiling heat transfer to formic acid, propanol and 2-butanol pure liquids under the atmospheric pressure
35. Nikkhah V, Sarafraz MM, Hormozi F (2015) Application of spherical copper oxide (II) water nano-fluid as a potential coolant in a boiling annular heat exchanger. *Chem Biochem Eng Q* 29:405–415
36. Arya A, Sarafraz MM, Shahmiri S, Madani SAH, Nikkhah V, Nakhjavani SM (2018) Thermal performance analysis of a flat heat pipe working with carbon nanotube-water nanofluid for cooling of a high heat flux heater. *Heat Mass Transf* 54:985–997
37. Sarafraz MM, Nikkhah V, Nakhjavani M, Arya A (2018) Thermal performance of a heat sink microchannel working with biologically produced silver-water nanofluid: experimental assessment. *Exp Thermal Fluid Sci* 91:509–519
38. Sahin B, Gültekin GG, Manay E, Karagoz S (2013) Experimental investigation of heat transfer and pressure drop characteristics of Al₂O₃-water nanofluid. *Exp Thermal Fluid Sci* 50:21–28. <https://doi.org/10.1016/j.expthermflusci.2013.04.020>
39. Wang J, Zhu J, Zhang X, Chen Y (2013) Heat transfer and pressure drop of nanofluids containing carbon nanotubes in laminar flows. *Exp Thermal Fluid Sci* 44:716–721
40. Fazeli SA, Hashemi SMH, Zirakzadeh H, Ashjaee M (2012) Experimental and numerical investigation of heat transfer in a miniature heat sink utilizing silica nanofluid. *Superlattice Microst* 51:247–264
41. M.M. Sarafraz, J. Hart, E. Shrestha, H. Arya, M. Arjomandi, (2019) Experimental thermal energy assessment of a liquid metal eutectic in a microchannel heat exchanger equipped with a (10 Hz/50 Hz) resonator. *Applied Thermal Engineering* 148:578-590
42. M.M. Sarafraz, M.R. Safaei, (2019) Diurnal thermal evaluation of an evacuated tube solar collector (ETSC) charged with graphene nanoplatelets-methanol nano-suspension. *Renewable Energy* 142: 364-372
43. Moffat RJ (1988) Describing the uncertainties in experimental results. *Exp Thermal Fluid Sci* 1:3–17
44. Kline SJ, McClintock F (1953) Describing uncertainties in single-sample experiments. *Mech Eng* 75:3–8
45. El Bécaye Maïga S, Tam Nguyen C, Galanis N, Roy G, Maré T, Coqueux M (2006) Heat transfer enhancement in turbulent tube flow using Al₂O₃ nanoparticle suspension. *International Journal of Numerical Methods for Heat & Fluid Flow* 16:275–292
46. Sarafraz MM (2012) Nucleate pool boiling of aqueous solution of citric acid on a smoothed horizontal cylinder. *Heat Mass Transf* 48: 611–619
47. Sarafraz MM, Peyghambarzadeh SM (2012) Nucleate pool boiling heat transfer to Al₂O₃-water and TiO₂-water nanofluids on horizontal smooth tubes with dissimilar homogeneous materials. *Chem Biochem Eng Q* 26:199–206
48. Sarafraz MM, Peyghambarzadeh SM, Alavifazel SA (2012) Enhancement of nucleate pool boiling heat transfer to dilute binary mixtures using endothermic chemical reactions around the smoothed horizontal cylinder. *Heat Mass Transf* 48:1755–1765
49. Peyghambarzadeh SM, Sarafraz MM, Vaeli N, Ameri E, Vatani A, Jamialahmadi M (2013) Forced convective and subcooled flow boiling heat transfer to pure water and n-heptane in an annular heat exchanger. *Ann Nucl Energy* 53:401–410

Publisher's note Springer Nature remains neutral with regard to jurisdictional claims in published maps and institutional affiliations.